

## Crystal Structure of the Triterpenoid Baccharis Oxide: with a Note on the Use of Various Approaches in the Tangent-Refinement Procedure

BY FRODE MO

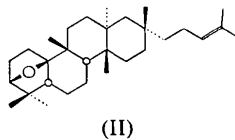
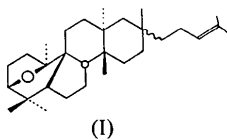
Institutt for röntgenteknikk, Universitetet i Trondheim-NTH, N-7034 Trondheim-NTH, Norway

(Received 23 March 1973; accepted 26 March 1973)

Baccharis oxide,  $C_{30}H_{50}O$ , crystallizes in space group  $P2_12_12_1$ , with  $a=7.413$  (1),  $b=11.866$  (2),  $c=29.067$  (10) Å,  $Z=4$ . The structure was solved by direct methods. Two different procedures for developing phases by the tangent formula have been used and the results are discussed. Least-squares refinement converged at an  $R$  of 0.043 based on 1971  $F_{obs}$  ( $R_w=0.044$ ). An oxide bridge between C(3) and C(10) in the six-membered ring  $A$  makes this structure a novel one among the triterpenes. Repulsion between 1,3-diaxial substituents enhances the steric strain in the fused-ring system. The 1,3 contacts are responsible for a pronounced flattening and twisting of the *trans*-fused rings  $C$  and  $D$ . The molecular structure is largely determined by intramolecular factors. Efficient stacking of molecules in the crystal is accomplished by van der Waals interactions.

### Introduction

The title compound was first isolated from the roots of *Baccharis halimifolia* L. by Anthonsen *et al* (1970). They suggested formula (I) for the constitution and partial stereochemistry from chemical and spectroscopic evidence. The proposed model, for which the configuration at C(17) was assigned later (Suokas & Hase, 1971), shows baccharis oxide to be a new type of triterpenoid structure. As there was still some doubt as to the structural details of ring  $A$ , an X-ray investigation was undertaken and the correct structure was shown to be (II).



Preliminary photographs were of very good quality and it was hoped that the X-ray analysis might also provide fairly precise parameters for the triterpenoid molecule.

When this work was initiated a program for the direct determination of phases in non-centrosymmetric space groups was being written at this Institute. The structure of baccharis oxide was to serve as a test case for an unbiased comparison of various approaches in the process of accepting new phases from the tangent formula.

A preliminary note on this work has already been published (Mo, Anthonsen & Bruun, 1972).

### Experimental

#### Crystal data

Crystals of baccharis oxide grown from a petroleum solution were kindly supplied by Dr T. Bruun, Organic Chemical Laboratories of this University. Oscillation

and Weissenberg photographs showed orthorhombic symmetry. The systematic extinctions among the axial reflexions were those of space group  $P2_12_12_1$ . Crystallographic data are summarized below.

Baccharis oxide,  $C_{30}H_{50}O$ ; F.W. 426.73; m.p. 148–149°C  
 $a = 7.413$  (1) Å  
 $b = 11.866$  (2) Å  
 $c = 29.067$  (10) Å  
 $\lambda_{Cu K\alpha_1} = 1.5405$  Å  
 $V = 2556.8$  Å<sup>3</sup>  
 $D_x = 1.108$  g cm<sup>-3</sup> for  $Z = 4$   
 $\mu(Cu K\alpha) = 4.8$  cm<sup>-1</sup>.

Orthorhombic, systematic extinctions:  $h00$  when  $h$  odd,  $0k0$  when  $k$  odd and  $00l$  when  $l$  odd.  
 Space group:  $P2_12_12_1$ .

Cell dimensions were determined by a least-squares fit to the setting angles measured for 12 high-angle reflexions. The determination was repeated after 9 days and at the end of data collection *i.e.* 14 days. The values found for  $c$ : 29.057 (2) Å (start), 29.075 (3) Å (after 9 days) and 29.093 (2) Å (end) show a systematic increase. The value 29.067 (10) Å should represent  $c$  fairly well halfway in the data collection, and the error given is about four times larger than that obtained in a single determination. Variations in  $a$  and  $b$  were insignificant and not systematic.

A crystal of dimensions 0.13 × 0.17 × 0.20 mm was mounted with its longest dimension,  $a$ , approximately parallel to the goniometer  $\varphi$  axis.

#### Data collection and processing

Data were collected on a Picker FACS-1 four-circle diffractometer with Ni-filtered  $Cu K\alpha$  radiation and a scintillation counter. Intensities of 4813 reflexions of the classes  $hkl$  and  $hk\bar{l}$  (systematic extinctions not included) accessible below  $2\theta = 129^\circ$  were measured with the  $\omega/2\theta$  scan technique, a take-off angle of  $3.5^\circ$  and a

scan rate in  $2\theta$  of  $1^\circ \text{ min}^{-1}$ . A basic scan range of  $1.3^\circ$  to be appropriately corrected for dispersion was chosen from  $\omega$ -scan checks of the mosaic spread of the crystal. The counting rate was kept below *ca.*  $10^4$  c.p.s. by means of attenuators. Background was measured for 40 sec at each end of the scan. Two standard reflexions, 024 and 132, were measured every 20 reflexions. Their intensities showed maximum long-term variations of *ca.* 1.5% around their mean values. The 024 intensity remained virtually constant during the data collection whereas the intensity of 132 decreased systematically to about 96% of its initial value. The sum of the net counts for the standards was used to scale the data in conjunction with the usual Lorentz and polarization correction. No absorption correction was made ( $\mu R$ : 0.035–0.06).

2453 independent reflexions, including zero observations, were used for the structure determination and initial refinement. Mainly because of the small crystal size, there was a relatively high fraction of weak intensities, and 443 reflexions or 18% of the data had  $\sigma(I) \geq I$  where:

$$I = I_{\text{tot}} - TB = \text{net intensity}$$

$$\sigma(I) = (I_{\text{tot}} + T^2B)^{1/2}.$$

$I_{\text{tot}}$  is the total number of counts in the peak,  $B$  is the total number of counts in the backgrounds, and  $T$  is the ratio between scan time over the peak and total scan time over the backgrounds.

The two data sets  $hkl$  and  $h\bar{k}\bar{l}$  are in principle not equivalent in space group  $P2_12_12_1$ . The anomalous dispersion corrections for oxygen and carbon are rather small, however; for O:  $\Delta f' = 0.047$ ,  $f'' = 0.032$ ; and C:  $\Delta f' = 0.017$ ,  $f'' = 0.009$  (after Cromer & Liberman, 1970). Therefore, very accurate data, implying generally low  $\sigma(I)$ 's, are needed in order to take advantage of anomalous dispersion effects in this case. An estimate of the expectation value of the normalized Bijvoet ratio  $\langle |X| \rangle$  can be made according to Zachariasen (1965).  $X_H$  is defined as:  $(I_H - I_{\bar{H}})/\frac{1}{2}(I_H + I_{\bar{H}})$  where  $H \equiv hkl$ . With  $\lambda \text{Cu K}\alpha$  one calculates for  $2\theta \sim 100^\circ$ :  $\langle |X| \rangle \sim 0.6\%$  and for  $2\theta \sim 55^\circ$ :  $\langle |X| \rangle \sim 0.3\%$ . Since the intensity differences for most Bijvoet pairs will not be measurable, the average of the intensities of pairs  $hkl$  and  $h\bar{k}\bar{l}$  was taken. A new  $\sigma(F)$  was calculated as:

$$\sigma(F)_N = [1/\sigma^2(F_H) + 1/\sigma^2(F_{\bar{H}})]^{-1/2},$$

where

$$\sigma(F_H) = \frac{1}{2} F_H [\sigma(I_H)/I_H].$$

### Structure determination

The structure was solved by direct methods (Karle & Karle, 1966) as adapted in local phasing programs (Mo, 1972). The programs set up relationships of the  $\Sigma_2$  type (Hauptman & Karle, 1953), and assign and refine phases by means of the tangent formula (Karle & Hauptman, 1956) which is applied in a recycling

manner. Some of the phases in a starting set are permuted in steps of *e.g.*  $\pi/4$  and for each phase combination the phase model of all  $E$ 's above some preset limit is developed.

### Description of programs

Two different procedures for developing phases were compared in this work. In one of the versions (*TANGO*) new and refined phases are tested against a series of reject criteria before they can be accepted. Only a specified fraction  $f_z$  of the 'best' new phases from the last iteration cycle is considered further. 'Best' phases are those with the highest calculated values of  $Z_H$  as defined by Germain & Woolfson (1968). *Refined* phases that do not belong to the starting set are rejected if the last calculated phase shift exceeds some limiting value, *e.g.*  $120^\circ$ . If the number of  $\Sigma_2$  indications for any phase is below a preset figure  $n_s$  (*e.g.* 2 or 3) this reflexion is not accepted. A special test is carried out on zonal reflexions accepting only those for which the indicated phase is within a specified range, *e.g.*  $\pm 60^\circ$ , from the values permitted by the space-group symmetry. The nearest permitted phase values are used in the following cycle.

The fraction  $f_z$  can be varied between cycles, but for the last cycles  $f_z = 1.0$ . In some instances the  $n_s$  criterion had to be relaxed during the first cycles. Starting-set phases are allowed to refine only after a preset number of cycles.

Three different figures of merit are calculated for each phase model:

1.  $C = \sum_H Z_H$  (Germain & Woolfson, 1968).

2. Karle  $R$  index:  

$$R = \frac{\sum_H ||E_H|_o - |E_H|_c|}{\sum_H |E_H|_o}$$
 (Karle & Karle, 1966).

3. Average phase shift in last cycle:

$$DA = \langle |\varphi_{H \text{ new}} - \varphi_{H \text{ old}}| \rangle_H$$

In the other program version (*TANNY*) a reliability index  $\kappa_{HK}$  (Karle & Karle, 1966) is calculated for each indication of a phase  $\varphi_H$ . New phases are developed by means of the weighted tangent formula according to Germain, Main & Woolfson (1971):

$$\tan \varphi_H = \frac{\sum_K w_K w_{H-K} |E_K E_{H-K}| \sin(\varphi_K + \varphi_{H-K})}{\sum_K w_K w_{H-K} |E_K E_{H-K}| \cos(\varphi_K + \varphi_{H-K})} = \frac{N_H}{D_H},$$

where the weight of a general phase is related to its variance:

$$w_H = \tanh(\frac{1}{2}\alpha_H) = \tanh[\sigma_3 \sigma_2^{-3/2} |E_H| (N_H^2 + D_H^2)^{1/2}].$$

For zonal reflexions *TANNY* calculates the weight as:

$$w'_H = \text{AMAX} \{ \frac{1}{4} [1 + 3 \cos(\Delta\varphi_H)], w_H \}.$$

$\Delta\varphi_H$  is the deviation between the calculated phase value

and the nearest permitted value. The latter is used for  $\varphi_H$  in the following cycle.

The development of phases in *TANNY* is similar to that used in the program *MULTAN* (Germain, Main & Woolfson, 1971). Thus, in contrast to the procedure in *TANGO* all new or refined phases are accepted from the modified tangent formula. Their relative reliability is taken into account by weighting them differently. The starting set consists of: (a) phases for fixing the origin and enantiomorph – weight = 1.0, (b) phases (signs) of centric reflexions from  $\Sigma_1$  relations (Hauptman & Karle, 1953) – initial weight =  $2P - 1$  where  $P$  is probability of sign, (c) phases of a small number of selected reflexions – weight = 1.0.

Four figures of merit are used to characterize each phase model:

1. Karle  $R$  index.
2. Germain-Main-Woolfson  $AM$  index:

$$AM = \frac{\sum_H \alpha_H - \sum_H \alpha_{H \text{ rand}}}{\sum_H \alpha_{H \text{ est}} - \sum_H \alpha_{H \text{ rand}}}$$

(Germain, Main & Woolfson, 1971).

3. Sum over  $\alpha$ 's after last cycle:

$$SA = \sum_H \alpha_H.$$

4.  $DA$ .

#### Comparison of methods

Some 40 phase models were developed altogether with *TANGO* starting from three different sets of reflexions. The models with the lowest  $R$  indices and highest values of  $C$  were examined more extensively from  $E$  maps, but none of them gave the correct model. Two starting sets of reflexions were tested with *TANNY*, and the correct structure was eventually found from the set given below:

$hkl$	$E$	$\varphi$	$w$	
*0 3 15	2.47	$\pi/2$	1.	} Origin
*2 5 0	2.54	0	1.	
*5 6 0	3.04	$\pi/2$	1.	
*0 8 17	2.64	$\pi$	1.	} Enantiomorph
*0 8 10	2.82	$\pi$	0.56	
2 12 0	1.81	0	0.60	} From $\Sigma_1$
6 4 0	2.01	$\pi$	0.52	
2 5 1	2.05	$\pm \pi/4$ $\pm \pi/2$ $\pm 3\pi/4$	1.	
4 2 18	2.43	$\pm \pi/4$ $\pm 3\pi/4$	1.	

A set of 275  $E$ 's  $\geq 1.50$  were phased from the starting set with phases  $+\pi/4$  and  $-\pi/4$  for reflexions 251 and 4,2,18. The  $E$  map for this model (2.13) showed clearly the heavier atoms of the structure, except C(2) and six of the carbon atoms in the chain, *i.e.* 24 atoms.

It was then realized that model 2.13 could be compared with model 17 obtained previously with *TANGO*. Reflexions 1,10,0 ( $\varphi = -\pi/2$ ) and 1,8,18 ( $\varphi = +\pi/2$ ) had been used in addition to the starred reflexions and

phases shown above to develop model 17. However, the correct structure was not identified in the corresponding  $E$  map, even though it was found later that nine of the 24 atomic peaks in the 2.13 map had also been marked as peaks in the 17 map. On the other hand there were several false maxima, medium and strong, that conformed well to five- and six-membered rings. Thus, in the most probable nine-atom partial structure from this map there were only two approximately correct atomic positions. The average phase difference  $\langle |\delta\varphi| \rangle$  for 211  $E$ 's  $\geq 1.60$  in the two models was  $37^\circ$ .

For a more systematic comparison both programs were used to develop phases within a selected set of 100 reflexions always, starting from sets of five phases. The final  $\langle |\delta\varphi| \rangle$  varied but was in one instance as large as  $82.5^\circ$ . Such occasional divergence could be attributed to the different principles employed in *TANGO* and *TANNY*. Another possible explanation is the low number of phases in the starting sets. The importance of the latter point was apparent in another series of runs in which *TANGO* was used both in the usual way and semi-manually, *i.e.* new phases are accepted upon inspection of the results between cycles. With seven phases in the starting set there was in general good correlation between pairs of phase models. With five starting phases larger discrepancies occurred, the largest  $\langle |\delta\varphi| \rangle$  being  $80^\circ$ .

Summing up the results of these tests, one concludes that the principle of applying a series of reject criteria for accepting phases from the tangent formula may in itself introduce hazards, contrary to what was intended. The size of the starting set is an important parameter and the results above should not be taken to imply that a set of seven phases will always be adequate for this size of structure. A principal advantage of the phase-accepting procedure in *TANNY*, which is quite similar to that used in *MULTAN*, is the rapid generation of more phases starting from a largest possible set of phases. The principles in *TANNY* imply a quicker convergence than with *TANGO*. As a result *TANNY* is faster than *TANGO* by a factor of two.

#### Structure refinement

All C and O atoms were found from a difference Fourier map calculated from the 24-atom model ( $R = 0.41$ ) in the  $E$  map of model 2.13. Full-matrix least-squares isotropic refinement based on 2453 unweighted reflexions including zero observations converged quickly at an  $R = 0.149$  ( $R = \sum |F_o| - K|F_c| / \sum |F_o|$ ). All 50 hydrogen atoms were then located in a difference map. Continued isotropic refinement reduced  $R$  to 0.097. After one more cycle with anisotropic temperature factors for carbon and oxygen  $R$  was 0.069. Averaged  $F_o$ 's and new values for the errors  $\sigma(F_o)_N$  were calculated, *cf.* *Data collection and processing*, and 1951 reflexions with  $F_o \geq 3\sigma(F_o)_N$  were considered observable. 20 reflexions with  $3\sigma(F_o)_N >$

F\_0 >= 2 sigma(F\_0)\_N had F\_c > F\_0. They were included with a secondary extinction was observed. A correction for this new F\_0 set at 3 sigma(F\_0)\_N. Among the strongest intensities, effect according to Zachariasen (1963) was made for systematic weakening that might be ascribed to sec-

Table 1. Observed and calculated structure factors

The columns are I, 100F\_0 and 100F\_c respectively.

Table with multiple columns containing numerical data for various indices and structure factors. The table is organized into several sections, each with a header row indicating the column group. The data consists of integers and some floating-point numbers, representing observed and calculated structure factors for different reflections.

of least-squares reduced  $R$  to 0.045. The final weighting scheme was:  $1/w = \sigma^2$ , where  $\sigma^2 = [\sigma^2(F_o)_N + cF_o^2]$ .  $c$  was determined as  $5.0 \cdot 10^{-4}$  from an analysis of  $\langle w(F_o - KF_o)^2 \rangle$  with groups of increasing  $F_o$ .

Refinement was continued until all parameter shifts

were less than 0.3 of the corresponding e.s.d.'s. The final  $R$  and  $R_w$ , defined as:  $R_w = [\sum w(|F_o| - K|F_c|)^2 / \sum wF_o^2]^{1/2}$  and based on 1971 observed reflexions were:  $R = 0.043$  and  $R_w = 0.044$ .

Atomic form factors used were: C and O, Doyle &

Table 2. Final atomic parameters of baccharis oxide

Thermal parameters,  $U_{ij} (\times 10^4)$ , as given here are defined by:

$$\exp[-2\pi^2(U_{11}a^2h^2 + U_{22}b^2k^2 + U_{33}c^2l^2 + 2U_{12}a^*b^*hk + 2U_{13}a^*c^*hl + 2U_{23}b^*c^*kl)].$$

E.s.d.'s of the parameters appear in parentheses. The H atoms are identified by the number of the attached C atom.

	$x$	$y$	$z$	$U_{11}$	$U_{22}$	$U_{33}$	$U_{12}$	$U_{13}$	$U_{23}$
O	0.3977 (3)	0.2323 (1)	0.2190 (1)	662 (14)	549 (11)	363 (9)	6 (12)	-4 (10)	16 (5)
C(1)	0.6138 (5)	0.2240 (3)	0.1624 (1)	514 (21)	714 (24)	555 (20)	8 (21)	-10 (17)	-64 (11)
C(2)	0.6905 (5)	0.2889 (3)	0.2044 (1)	576 (22)	934 (25)	703 (21)	8 (21)	-64 (17)	-164 (12)
C(3)	0.5188 (4)	0.3252 (3)	0.2284 (1)	747 (23)	639 (19)	440 (15)	-27 (20)	-16 (16)	-66 (9)
C(4)	0.4221 (5)	0.4240 (5)	0.2046 (1)	808 (26)	548 (18)	492 (16)	-93 (20)	123 (18)	-50 (9)
C(5)	0.3655 (4)	0.3629 (2)	0.1590 (1)	586 (19)	448 (15)	419 (15)	-38 (16)	123 (14)	12 (8)
C(6)	0.1748 (5)	0.3821 (2)	0.1424 (1)	721 (24)	468 (16)	623 (18)	147 (17)	81 (17)	13 (9)
C(7)	0.1373 (4)	0.3127 (2)	0.0989 (1)	527 (19)	483 (17)	655 (18)	118 (17)	-51 (17)	17 (9)
C(8)	0.2391 (4)	0.1986 (2)	0.0968 (1)	348 (16)	422 (15)	462 (14)	14 (15)	-26 (13)	42 (7)
C(9)	0.2799 (4)	0.1503 (2)	0.1458 (1)	430 (17)	407 (14)	449 (14)	26 (14)	41 (14)	30 (8)
C(10)	0.4092 (4)	0.2373 (2)	0.1689 (1)	470 (18)	512 (16)	386 (13)	27 (16)	67 (14)	11 (8)
C(11)	0.3687 (4)	0.0324 (2)	0.1413 (1)	660 (20)	472 (15)	426 (14)	103 (17)	-88 (15)	69 (8)
C(12)	0.2763 (4)	-0.0463 (2)	0.1076 (1)	619 (21)	379 (14)	530 (15)	-12 (16)	-61 (16)	48 (8)
C(13)	0.2670 (4)	0.0052 (2)	0.0591 (1)	453 (17)	395 (14)	438 (15)	4 (14)	-19 (14)	36 (8)
C(14)	0.1538 (4)	0.1157 (2)	0.0615 (1)	388 (16)	413 (14)	485 (14)	6 (13)	-42 (13)	46 (7)
C(15)	0.1550 (4)	0.1662 (2)	0.0126 (1)	488 (18)	484 (16)	495 (15)	65 (16)	-87 (14)	43 (8)
C(16)	0.0657 (4)	0.0894 (3)	-0.0228 (1)	599 (22)	624 (18)	528 (15)	113 (19)	-157 (16)	28 (10)
C(17)	0.1248 (4)	-0.0360 (2)	-0.0230 (1)	597 (20)	510 (16)	465 (15)	-80 (18)	-97 (16)	22 (8)
C(18)	0.1745 (4)	-0.0788 (2)	0.0261 (1)	587 (21)	410 (15)	517 (15)	-47 (16)	-92 (16)	33 (8)
C(19)	0.2792 (5)	-0.0510 (2)	-0.0587 (1)	750 (24)	480 (16)	501 (16)	-55 (18)	-87 (17)	34 (9)
C(20)	0.3747 (5)	-0.1651 (2)	-0.0599 (1)	859 (25)	544 (17)	537 (17)	31 (21)	25 (25)	11 (11)
C(21)	0.4778 (5)	-0.1836 (3)	-0.1037 (1)	765 (24)	554 (18)	567 (17)	-36 (20)	22 (17)	51 (10)
C(22)	0.4237 (5)	-0.2393 (2)	-0.1405 (1)	782 (24)	488 (16)	540 (16)	86 (19)	8 (17)	39 (9)
C(23)	0.5399 (6)	-0.2492 (3)	-0.1829 (1)	1146 (33)	866 (25)	597 (20)	-44 (28)	99 (21)	64 (12)
C(24)	0.2465 (6)	-0.2992 (3)	-0.1437 (1)	885 (29)	962 (27)	980 (26)	-92 (28)	-99 (25)	-121 (14)
C(25)	-0.0352 (5)	-0.1063 (3)	-0.0404 (1)	707 (25)	861 (25)	644 (20)	-203 (22)	-153 (18)	-21 (12)
C(26)	0.4620 (4)	0.0226 (2)	0.0425 (1)	494 (18)	456 (15)	565 (16)	47 (16)	-40 (14)	-14 (8)
C(27)	-0.0466 (4)	0.0917 (3)	0.0737 (1)	394 (19)	756 (21)	658 (18)	-14 (18)	-22 (16)	-3 (11)
C(28)	0.1087 (4)	0.1339 (2)	0.1763 (1)	562 (20)	653 (19)	590 (18)	-81 (18)	108 (17)	39 (10)
C(29)	0.5376 (6)	0.5279 (3)	0.1959 (1)	1342 (37)	741 (24)	690 (21)	-387 (28)	24 (25)	-72 (12)
C(30)	0.2616 (6)	0.4599 (3)	0.2344 (1)	1092 (31)	729 (21)	595 (19)	190 (26)	189 (21)	-48 (11)

	$x$	$y$	$z$	$B(\text{\AA}^2)$	$x$	$y$	$z$	$B(\text{\AA}^2)$	
H(11)	0.651 (4)	0.149 (2)	0.164 (1)	3.1 (0.6)	H(211)	0.603 (5)	-0.147 (2)	-0.105 (1)	7.0 (0.8)
H(12)	0.651 (4)	0.249 (2)	0.133 (1)	4.2 (0.7)	H(231)	0.575 (6)	-0.335 (3)	-0.192 (1)	10.3 (1.1)
H(21)	0.765 (5)	0.243 (3)	0.225 (1)	8.8 (0.9)	H(232)	0.657 (5)	-0.209 (3)	-0.178 (1)	10.5 (1.0)
H(22)	0.753 (4)	0.364 (2)	0.195 (1)	6.6 (0.8)	H(233)	0.472 (5)	-0.211 (3)	-0.211 (1)	7.5 (0.9)
H(31)	0.526 (4)	0.335 (2)	0.262 (1)	5.2 (0.7)	H(241)	0.271 (7)	-0.376 (4)	-0.149 (2)	13.4 (1.4)
H(51)	0.448 (4)	0.391 (2)	0.136 (1)	4.3 (0.6)	H(242)	0.158 (8)	-0.287 (4)	-0.117 (2)	14.7 (1.6)
H(61)	0.094 (4)	0.359 (2)	0.168 (1)	5.4 (0.7)	H(243)	0.185 (6)	-0.275 (4)	-0.171 (2)	12.4 (1.4)
H(62)	0.154 (4)	0.468 (2)	0.135 (1)	6.4 (0.8)	H(251)	-0.020 (5)	-0.191 (3)	-0.041 (1)	7.8 (0.9)
H(71)	0.003 (3)	0.298 (2)	0.097 (1)	4.8 (0.6)	H(252)	-0.131 (4)	-0.098 (3)	-0.021 (1)	6.4 (0.7)
H(72)	0.175 (4)	0.359 (2)	0.071 (1)	4.8 (0.7)	H(253)	-0.067 (5)	-0.080 (3)	-0.072 (1)	7.1 (0.8)
H(81)	0.365 (3)	0.216 (2)	0.084 (1)	2.1 (0.5)	H(261)	0.531 (4)	-0.046 (3)	0.048 (1)	6.3 (0.8)
H(111)	0.372 (3)	-0.001 (2)	0.173 (1)	4.2 (0.6)	H(262)	0.469 (4)	0.046 (2)	0.008 (1)	5.1 (0.7)
H(112)	0.500 (4)	0.044 (2)	0.131 (1)	4.3 (0.6)	H(263)	0.519 (4)	0.078 (3)	0.060 (1)	5.7 (0.7)
H(121)	0.344 (4)	-0.118 (2)	0.107 (1)	4.2 (0.6)	H(271)	-0.093 (6)	0.046 (3)	0.054 (1)	8.7 (1.0)
H(122)	0.147 (4)	-0.063 (2)	0.117 (1)	3.7 (0.6)	H(272)	-0.067 (4)	0.068 (2)	0.106 (1)	6.3 (0.8)
H(151)	0.290 (3)	0.185 (2)	0.004 (1)	4.1 (0.6)	H(273)	-0.107 (7)	0.163 (4)	0.070 (1)	12.6 (1.3)
H(152)	0.090 (4)	0.240 (2)	0.012 (1)	4.8 (0.6)	H(281)	0.052 (4)	0.058 (2)	0.170 (1)	5.9 (0.7)
H(161)	-0.067 (4)	0.088 (2)	-0.018 (1)	4.7 (0.6)	H(282)	0.147 (5)	0.134 (3)	0.212 (1)	9.3 (1.1)
H(162)	0.085 (4)	0.123 (2)	-0.054 (1)	5.4 (0.7)	H(283)	0.024 (4)	0.199 (3)	0.172 (1)	7.4 (0.8)
H(181)	0.241 (4)	-0.147 (2)	0.024 (1)	4.2 (0.6)	H(291)	0.642 (4)	0.506 (2)	0.177 (1)	7.9 (0.8)
H(182)	0.050 (4)	-0.107 (2)	0.041 (1)	4.9 (0.7)	H(292)	0.573 (5)	0.562 (3)	0.224 (1)	9.5 (1.0)
H(191)	0.221 (4)	-0.034 (2)	-0.089 (1)	4.8 (0.6)	H(293)	0.452 (5)	0.589 (3)	0.178 (1)	8.5 (0.9)
H(192)	0.364 (3)	0.007 (2)	-0.054 (1)	3.9 (0.6)	H(301)	0.199 (4)	0.391 (3)	0.243 (1)	6.5 (0.8)
H(201)	0.283 (4)	-0.222 (2)	-0.059 (1)	5.3 (0.7)	H(302)	0.321 (5)	0.496 (3)	0.264 (1)	7.9 (0.9)
H(202)	0.460 (5)	-0.172 (3)	-0.032 (1)	9.6 (1.0)	H(303)	0.174 (4)	0.514 (2)	0.217 (1)	5.7 (0.7)

Turner (1968) and H (bonded) Stewart, Davidson & Simpson (1965). Observed and calculated structure factors are reproduced in Table 1.

*Analysis of thermal motion*

Least-squares analyses of the possible rigid-body motion of the molecule or a part of the molecule were made by the method of Schomaker & Trueblood (1968). An apparently good fit was obtained for a model consisting of the 19 C and O atoms in the ring system including atoms C(26), C(27) and C(28). The r.m.s. deviation of the experimental  $U_{ij}$ 's from those calculated from the **T**,  **$\omega$**  and **S** tensors is 0.0032 Å<sup>2</sup>;  $\sigma(U_{ij \text{ calc}})$  is 0.0035 Å<sup>2</sup>, and the mean value of  $\sigma(U_{ij \text{ exp}})$  is 0.0016 Å<sup>2</sup>.

The translational motion is small, ~0.20 Å, and very nearly isotropic. The librational motion is also small; the r.m.s. amplitudes are 3.9, 2.5 and 2.0° with the largest libration about an axis approximately parallel to the long axis of the molecule.

Rigid-body corrections of the apparent bond lengths (Cruickshank, 1956) are in the range 0.001 to 0.0045 Å with an average of 0.003 Å. The average e.s.d. of bonds between heavier atoms is 0.004 Å. These values are probably somewhat underestimated because of the necessary separation of variables into smaller groups during the least-squares refinement. The relative size of the calculated corrections is small. Moreover, since the experimental  $U_{ij}$ 's contain systematic errors of various origin that will affect the results of the rigid-body analysis, it was decided not to include possible thermal shifts in the final positional parameters (Table 2) and the calculated bond lengths (Table 3).

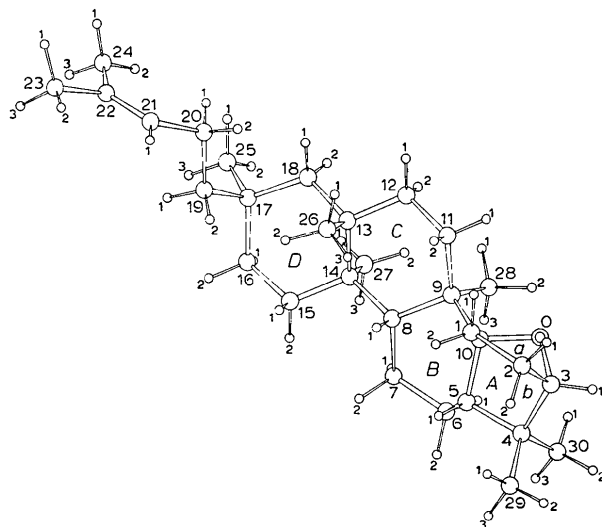


Fig. 1. Perspective view of the molecule down **a**. Large numerals are used for the numbering of oxygen (O) and carbon (1–30) atoms. Numbering of hydrogen atoms is in small numerals according to the system in Table 2.

Table 3. *Bond lengths*

E.s.d.'s of bonds between heavier atoms appear in parentheses. Bonds between secondary carbon atoms are marked with an asterisk.

O—C(3)	1.448 (4) Å	C(14)—C(8)	1.557 (4) Å
O—C(10)	1.459 (3)	C(14)—C(15)	1.542 (4)
*C(1)—C(2)	1.550 (5)	*C(15)—C(16)	1.526 (4)
C(1)—C(10)	1.537 (5)	C(16)—C(17)	1.551 (4)
C(2)—C(3)	1.515 (5)	C(17)—C(18)	1.560 (4)
C(3)—C(4)	1.539 (4)	C(17)—C(19)	1.555 (4)
C(4)—C(5)	1.568 (4)	*C(19)—C(20)	1.529 (4)
C(5)—C(6)	1.511 (5)	C(20)—C(21)	1.502 (4)
C(5)—C(10)	1.551 (4)	C(21)—C(22)	1.320 (4)
*C(6)—C(7)	1.533 (4)	C(22)—C(23)	1.508 (5)
C(7)—C(8)	1.551 (4)	C(22)—C(24)	1.496 (6)
C(8)—C(9)	1.565 (4)	C(4)—C(29)	1.522 (5)
C(9)—C(10)	1.561 (4)	C(4)—C(30)	1.531 (5)
C(9)—C(11)	1.551 (4)	C(9)—C(28)	1.561 (4)
*C(11)—C(12)	1.517 (4)	C(13)—C(26)	1.538 (4)
C(12)—C(13)	1.538 (4)	C(14)—C(27)	1.554 (4)
C(13)—C(14)	1.559 (4)	C(17)—C(25)	1.536 (5)
C(13)—C(18)	1.543 (4)		
C(1)—H(11)	0.93	C(21)—H(211)	1.02
C(1)—H(12)	0.95	C(23)—H(231)	1.08
C(2)—H(21)	0.97	C(23)—H(232)	1.00
C(2)—H(22)	1.04	C(23)—H(233)	1.06
C(3)—H(31)	0.99	C(24)—H(241)	0.95
C(5)—H(51)	0.96	C(24)—H(242)	1.02
C(6)—H(61)	1.00	C(24)—H(243)	0.96
C(6)—H(62)	1.05	C(25)—H(251)	1.02
C(7)—H(71)	1.01	C(25)—H(252)	0.92
C(7)—H(72)	1.03	C(25)—H(253)	1.01
C(8)—H(81)	1.02	C(26)—H(261)	0.98
C(11)—H(111)	1.01	C(26)—H(262)	1.05
C(11)—H(112)	1.03	C(26)—H(263)	0.93
C(12)—H(121)	0.98	C(27)—H(271)	0.86
C(12)—H(122)	1.01	C(27)—H(272)	1.00
C(15)—H(151)	1.05	C(27)—H(273)	0.96
C(15)—H(152)	1.00	C(28)—H(281)	1.01
C(16)—H(161)	0.99	C(28)—H(282)	1.06
C(16)—H(162)	1.01	C(28)—H(283)	1.00
C(18)—H(181)	0.95	C(29)—H(291)	0.99
C(18)—H(182)	1.08	C(29)—H(292)	0.94
C(19)—H(191)	1.01	C(29)—H(293)	1.09
C(19)—H(192)	0.94	C(30)—H(301)	0.97
C(20)—H(201)	0.96	C(30)—H(302)	1.05
C(20)—H(202)	1.03	C(30)—H(303)	1.05

**Results and discussion**

A view down **a** of one of the possible enantiomers of baccharis oxide is shown in Fig. 1. The ring nucleus consists of four six-membered rings labelled from **A** to **D** and two five-membered rings **a** and **b**.

*Bond lengths and angles*

Bond lengths and valency angles are given in Tables 3 and 4 with their e.s.d.'s ( $\sigma$ ), [see also Fig. 2(a) and (b)]. Bonds between formally  $sp^3$ -hybridized carbon atoms are in the range 1.511–1.568 Å ( $\sigma_{\text{mean}} \sim 0.004$  Å). There are five bonds between secondary carbon atoms marked with an asterisk in Table 3. Their average length, 1.531 Å, compares well with the normal value for a  $C(sp^3)$ – $C(sp^3)$  bond. The deviation of the C(1)–C(2) distance from 1.531 Å is significant and is probably related to the steric requirements of the atoms forming the five-membered ring **a**. The average length

of 24 C—C bonds involving tertiary and/or quaternary atoms is 1.546 Å. This is a normal value for the fused-ring systems in triterpenes or in steroids, *cf.* also the value 1.545 Å in diamond. There are, however, significant differences from the average within this group of bonds.

The C(21)—C(22) double bond in the C(17) side chain is 1.320 (4) Å and the three neighbouring C(sp<sup>2</sup>)—C(sp<sup>3</sup>) bonds range from 1.496 (6) to 1.508 (4) Å with

a mean of 1.502 Å. The two C(sp<sup>3</sup>)—O bonds are 1.448 (4) and 1.459 (3) Å, which are slightly but probably not significantly different. The longer bond involves the quaternary carbon atom C(10). The mean value, 1.454 Å, can be compared with the value 1.445 Å found in  $\alpha$ -2-ethyl-5-methyl-3,3-diphenyltetrahydrofuran (Singh & Ahmed, 1969) where both carbon atoms bonded to oxygen are tertiary.

The fifty C—H bonds, except one at 0.86 Å, fall in

Table 4. *Valency angles involving only carbon and oxygen atoms*

E.s.d.'s of the angles appear in parentheses.

C(3)—O—C(10)	97.0 (2) <sup>o</sup>	C(5)—C(10)—C(9)	115.4 (2) <sup>o</sup>
C(2)—C(1)—C(10)	102.4 (3)	C(9)—C(11)—C(12)	114.7 (2)
C(1)—C(2)—C(3)	101.3 (3)	C(11)—C(12)—C(13)	111.6 (2)
O—C(3)—C(2)	102.5 (2)	C(12)—C(13)—C(14)	108.5 (2)
O—C(3)—C(4)	101.8 (2)	C(12)—C(13)—C(18)	109.4 (2)
C(2)—C(3)—C(4)	113.6 (3)	C(12)—C(13)—C(26)	107.3 (2)
C(3)—C(4)—C(5)	98.8 (2)	C(14)—C(13)—C(18)	109.4 (2)
C(3)—C(4)—C(29)	115.4 (3)	C(14)—C(13)—C(26)	114.0 (2)
C(3)—C(4)—C(30)	108.6 (2)	C(18)—C(13)—C(26)	108.1 (2)
C(5)—C(4)—C(29)	112.6 (2)	C(8)—C(14)—C(13)	110.0 (2)
C(5)—C(4)—C(30)	113.5 (3)	C(8)—C(14)—C(15)	111.1 (2)
C(29)—C(4)—C(30)	107.8 (3)	C(8)—C(14)—C(27)	110.7 (2)
C(4)—C(5)—C(6)	116.7 (3)	C(13)—C(14)—C(15)	106.4 (2)
C(4)—C(5)—C(10)	103.4 (2)	C(13)—C(14)—C(27)	111.7 (2)
C(6)—C(5)—C(10)	113.5 (2)	C(15)—C(14)—C(27)	106.7 (2)
C(5)—C(6)—C(7)	110.6 (2)	C(14)—C(15)—C(16)	112.7 (2)
C(6)—C(7)—C(8)	114.4 (2)	C(15)—C(16)—C(17)	117.0 (2)
C(7)—C(8)—C(9)	112.2 (2)	C(16)—C(17)—C(18)	112.1 (2)
C(7)—C(8)—C(14)	112.3 (2)	C(16)—C(17)—C(19)	108.7 (2)
C(9)—C(8)—C(14)	116.6 (2)	C(16)—C(17)—C(25)	107.7 (3)
C(8)—C(9)—C(10)	105.5 (2)	C(18)—C(17)—C(19)	113.6 (3)
C(8)—C(9)—C(11)	109.6 (2)	C(18)—C(17)—C(25)	107.9 (2)
C(8)—C(9)—C(28)	113.9 (2)	C(19)—C(17)—C(25)	106.7 (2)
C(10)—C(9)—C(11)	111.9 (2)	C(13)—C(18)—C(17)	117.6 (2)
C(10)—C(9)—C(28)	109.7 (2)	C(17)—C(19)—C(20)	117.2 (2)
C(11)—C(9)—C(28)	106.4 (2)	C(19)—C(20)—C(21)	112.6 (2)
O—C(10)—C(1)	100.1 (2)	C(20)—C(21)—C(22)	127.3 (3)
O—C(10)—C(5)	102.2 (2)	C(21)—C(22)—C(23)	121.9 (3)
O—C(10)—C(9)	111.5 (2)	C(21)—C(22)—C(24)	123.7 (3)
C(1)—C(10)—C(5)	106.4 (3)	C(23)—C(22)—C(24)	114.5 (3)
C(1)—C(10)—C(9)	119.0 (3)		

Table 5. *Torsion angles in the rings*

$\varphi(y-z)^*$  is the abbreviation for  $\varphi(x-y-z-w)$ , the torsion angle about the  $y-z$  bond. The sequence  $x-y-z-w$  denotes bonded atoms where  $x$  and  $z$  belong to the ring in question.

Ring a		Ring b		Ring A	
Bond	$\varphi(y-z)$	Bond	$\varphi(y-z)$	Bond	$\varphi(y-z)$
C(1)—C(2)	+1.6 <sup>o</sup>	C(4)—C(5)	+9.7 <sup>o</sup>	C(1)—C(2)	+1.6 <sup>o</sup>
C(2)—C(3)	+33.6	C(5)—C(10)	+25.5	C(2)—C(3)	-75.5
C(3)—O	-57.2	C(10)—O	-52.4	C(3)—C(4)	+66.7
O—C(10)	+57.0	O—C(3)	+60.5	C(4)—C(5)	+9.7
C(10)—C(1)	-35.7	C(3)—C(4)	-42.8	C(5)—C(10)	-79.0
				C(10)—C(1)	+70.3
Ring B		Ring C		Ring D	
Bond	$\varphi(y-z)$	Bond	$\varphi(y-z)$	Bond	$\varphi(y-z)$
C(5)—C(6)	-57.2 <sup>o</sup>	C(8)—C(9)	+44.2 <sup>o</sup>	C(13)—C(14)	-62.9 <sup>o</sup>
C(6)—C(7)	+32.5	C(9)—C(11)	-46.5	C(14)—C(15)	+62.5
C(7)—C(8)	+28.0	C(11)—C(12)	+57.6	C(15)—C(16)	-48.7
C(8)—C(9)	-63.5	C(12)—C(13)	-61.5	C(16)—C(17)	+32.7
C(9)—C(10)	+39.1	C(13)—C(14)	+57.3	C(17)—C(18)	-35.3
C(10)—C(5)	+19.2	C(14)—C(8)	-51.3	C(18)—C(13)	+52.0

\* The sign convention for  $\varphi$  is that of Klyne & Prelog (1960).

the range 0.92–1.09 Å. The mean length, 1.00 Å, ( $\sigma_{\text{mean}} \sim 0.04$  Å) shows the expected shortening compared with the spectroscopic value.

Endocyclic C–C–C angles in rings *a* and *b* range from 98.8 to 103.4°. The mean value of 101.6° ( $\sigma_{\text{mean}} \sim 0.2^\circ$ ) is the same for each ring. The C–O–C angle is

97.0°. There are 48 C–C–C angles at  $sp^3$ -hybridized carbon atoms not including the internal angles in rings *a* and *b*. Their mean value is 111.5° ( $\sigma_{\text{mean}} \sim 0.2^\circ$ ). The internal valency angles in the six-membered rings *B*, *C* and *D* vary from 105.5 to 117.6° with an average of 112.1°. This increase over the tetrahedral value is similar to that found in other fused-ring systems and is related to the general flattening of the cyclohexane rings as noted by *e.g.* Geise, Altona & Romers (1967). The seven endocyclic angles at quaternary carbon atoms C(9), C(13), C(14) and C(17) fall in a narrower range 105.5–112.1° with a lower mean value of 108.8°. The 79 valency angles of the type X–C( $sp^3$ )–H, where X=C,O, vary from 103.2 to 117.2° and the mean is 109.4° ( $\sigma_{\text{mean}} \sim 1.7^\circ$ ). The average magnitude of the H–C–H angles is 108.3° ( $\sigma_{\text{mean}} \sim 2.6^\circ$ ) with a variation of  $\pm 6.5^\circ$ .

### Molecular structure

Rings *A*, *a* and *b* in the structure form a tricyclic system where *a* and *b* share atoms C(3), O and C(10) in an oxide bridge. Atoms C(5) and C(10) are bonded to each other. These features make the triterpene skeleton unique. The conformation of the rings may be described roughly as follows: *A* boat, *B* twist-boat, *C* and *D* chairs, *a* and *b* envelopes. A closer examination of the bond and angle values shows that there are considerable distortions from this idealized picture. The most important factors responsible for bonding distortions are short-range steric strain due to close angular substituents (methyl groups and side chain), strains introduced by the junction of rings and possible long-range transmission of strain associated with the effects mentioned above. In the discussion to follow reference should be made to calculated torsion angles in the rings, Table 5, least-squares planes through various parts of the molecule and atomic distances from such planes, Table 6.

The atoms C(1), C(2), C(3) and C(10) deviate only slightly from planarity (planes *pa* and *pa1*, Table 6) with the oxygen atom 0.81 Å out of this plane. Ring *a* is thus quite close to the envelope or  $C_s$  conformation. A larger distortion towards the half-chair or  $C_2$  form is found in ring *b* (plane *pb1*).

Ring *A* is in the boat form with a certain amount of twist. The torsion angles in an ideal (non-flattened) six-membered boat are: 0, –60, +60, 0, –60, +60°. The average magnitude of the four ‘high’ torsion angles in *A* is 72.9°, *i.e.* considerably larger than the ideal value. Concomitant features are four internal valency angles well below 109.5°. Ring *B* adopts a distorted twist-boat conformation. Comparison with the torsion angles in a non-flattened twist-boat, *i.e.* +30, +30, –60, +30, +30, –60°, shows that the most severe deformations occur near atom C(10). This atom is at the junction of four different rings and the stereochemistry here is of some interest. The conformation about the bond C(5)–C(10) is *syn-periplanar* (Fig. 3) with a mean torsion angle  $\langle \phi \rangle$  of only +25.6°. A slightly

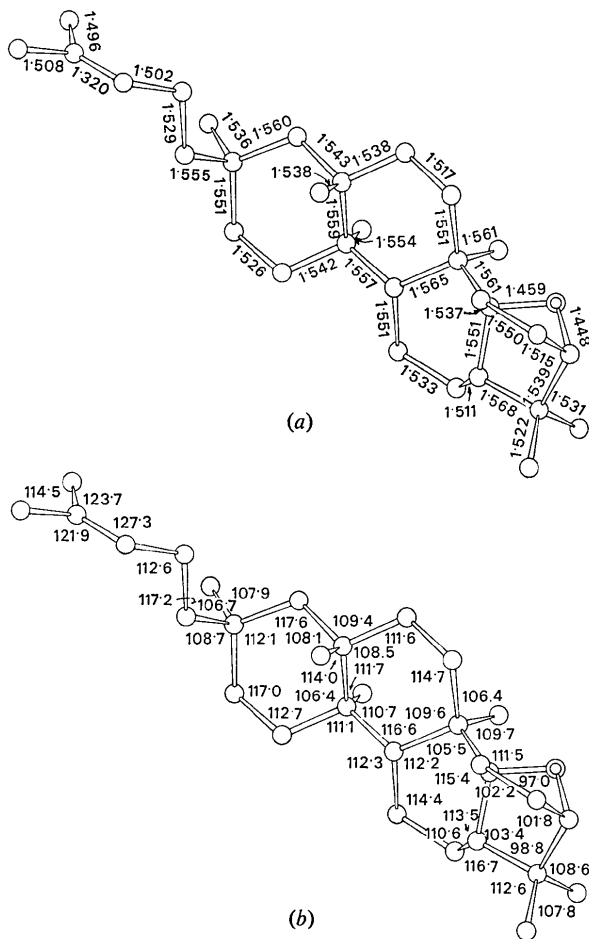


Fig. 2. Bond lengths (Å) and valency angles (°) in baccharis oxide. For valency angles not shown see Table 4.

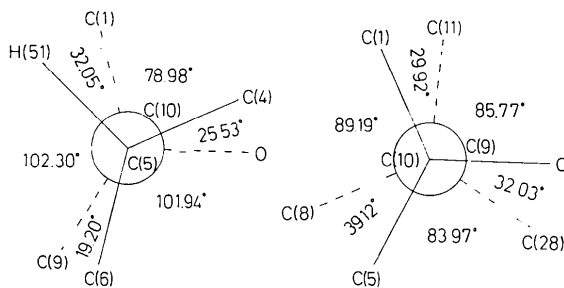


Fig. 3. Newman projections showing the conformation about the C(5)–C(10) and C(10)–C(9) bonds.



larger  $\langle\phi\rangle$  of  $+33.7^\circ$  exists about the C(10)–C(9) bond. These conformations bring about quite strong interactions across the bonds in question as can be seen from Table 7(a) and the C–C bonds in this region are generally long. A short contact H(11)···H(112) of  $\sim 1.94 \text{ \AA}$  is probably responsible for an increase of the angles C(1)–C(10)–C(9) and C(10)–C(9)–C(11). Similar arguments apply also to the opening of angle C(5)–C(10)–C(9).

The C and D rings are chairs in *trans* junction. In an undistorted system the bonds C(17)–C(19), C(13)–C(26), C(14)–C(27) and C(9)–C(28) would all be

parallel, separating pairs of atoms C(19) and C(26), C(27) and C(28) by only *ca.* 2.5 Å. This is much less than the distance expected from their van der Waals radius. The strain is relieved in part by a twist of the two rings and in part by an extra ring flattening. Both effects cause opening of the angles between the 1,3-diaxial C–C bonds. Ring D takes on a right-handed twist as seen from the bond C(13)–C(14) towards the C(16)–C(17) bond (plane *pD1*). There is a dihedral angle of  $9.9^\circ$  between the planes defined by atoms C(26)–C(13)–C(17) and C(13)–C(17)–C(19) and the opening angle between vectors C(13)–C(26) and C(17)–

Table 6. *Least-squares planes through various groups of atoms in the molecule*

The plane equations are of the form  $PX + QY + RZ = S$  where  $X$ ,  $Y$  and  $Z$  are expressed in Å relative to orthogonal axes parallel to  $a$ ,  $b$  and  $c$ .

Plane	Atoms	$P$	$Q$	$R$	$S$
<i>pa</i>	C(1)–C(2)–C(3)–C(10)	–0.0122	–0.8503	0.5261	0.1581
<i>pa1</i>	C(1)–C(2)–C(3)	0.0059	–0.8467	0.5320	0.2878
<i>pb</i>	C(3)–C(4)–C(5)–C(10)	–0.8707	–0.1709	0.4611	–0.9029
<i>pb1</i>	C(4)–C(5)–C(10)	–0.9226	–0.1303	0.3631	–1.3830
<i>pA</i>	C(1)–C(2)–C(4)–C(5)	–0.5383	–0.6187	0.5722	–1.4357
<i>pB</i>	C(5)–C(7)–C(8)–C(10)	–0.7396	–0.2301	0.6325	0.0701
<i>pC</i>	C(8)–C(9)–C(12)–C(13)	0.9918	0.0841	–0.0958	1.7445
<i>pC1</i>	C(9)–C(11)–MP	–0.8326	–0.4253	0.3549	–0.9819
<i>pD</i>	C(14)–C(15)–C(17)–C(18)	0.9930	0.0333	–0.1130	1.0725
<i>pD1</i>	C(16)–C(17)–MP	–0.8947	–0.2650	0.3597	–0.9554
<i>pF</i>	C(20)–H(211)–C(21)–C(22)–C(23)–C(24)	0.4098	–0.8329	0.3719	2.1392
<i>pR</i>	C(3) → C(18) except C(6)	–0.8990	–0.1126	0.4233	–0.7583

MP denotes the midpoint of the bond C(13)–C(14).

Deviations (Å) from least-squares planes.

	<i>pa</i>	<i>pa1</i>	<i>pb</i>	<i>pb1</i>	<i>pA</i>	<i>pB</i>	<i>pC</i>	<i>pC1</i>	<i>pD</i>	<i>pD1</i>	<i>pF</i>	<i>pR</i>
O	0.810	0.781	0.800	0.615								0.491
C(1)	0.010	0			0.043							–1.634
C(2)	–0.010	0			–0.042							–1.715
C(3)	0.007	0	–0.044	–0.257	0.777							–0.323
C(4)			0.061	0	0.041							–0.104
C(5)			–0.061	0	–0.043	–0.142						–0.207
C(6)						0.546						0.835
C(7)						0.142						0.643
C(8)						–0.143	–0.058					0.091
C(9)						0.665	0.058	0				0.486
C(10)	–0.007	–0.043	0.044	0	0.869	0.143						–0.208
C(11)							0.605	0				–0.004
C(12)							–0.059					0.302
C(13)							0.059	–0.083	0.701	–0.214		–0.301
C(14)							–0.669	0.083	–0.096	0.214		0.335
C(15)									0.093			–0.342
C(16)									–0.478	0		–0.080
C(17)									–0.092	0		–0.309
C(18)									0.096			0.021
C(19)											–1.422	–1.757
C(20)											–0.016	–2.255
C(21)											0.006	–3.457
C(22)											–0.005	–3.475
C(23)											–0.014	–4.757
C(24)											0.013	–2.252
C(25)												0.638
C(26)												–1.828
C(27)												1.853
C(28)												2.025
C(29)												–1.119
C(30)												1.284
H(211)											0.016	

C(19) is 27.7°. A left-handed twist is imposed on ring *C* as seen from the bond C(13)–C(14) towards the bond C(9)–C(11) (plane *pC1*). Because of close proximity of other atoms, in particular the oxygen atom, C(28) is forced 'back' so as to make the atomic sequence C(27)–C(14)–C(9)–C(28) significantly planar ( $\chi^2=0.01$ ). The opening angle between vectors C(14)–C(27) and C(9)–C(28) is 21.5°. The deformation of the rings makes the contacts C(19)···C(26) and C(27)···C(28) 3.356 and 3.237 Å. Similar distances between 1,3-diaxial methyl groups have been reported for  $\epsilon$ -caesalpin, 3.175 Å (Birnbaum & Ferguson, 1969), *p*-bromophenacyl labdanolate, 3.12 and 3.31 Å (Bjåmer, Ferguson & Melville, 1968), 3 $\beta$ -methoxy-21-keto- $\Delta^{13}$ -serratene, 3.34 and 3.35 Å (Allen & Trotter,

1970), adiantol B bromoacetate, 3.13 and 3.20 Å (Koyama & Nakai, 1970). Table 7(b) shows that 11 of the 14 shortest intramolecular H···H contacts involve hydrogens on axial carbon atoms C(19), C(26), C(27) and C(28). In fact, each of the axial methyl groups sits in a potential well surrounded by short 1,3 contacts. The accommodation of axial substituents thus seems to have a very strong influence on the whole molecular structure.

The flattening of ring *D* is very pronounced. Valency angles  $\theta$ [C(15)–C(16)–C(17)] and  $\theta$ [C(17)–C(18)–C(13)] are 117.0 and 117.6°, the corresponding torsion angles  $\phi$ [C(16)–C(17)] and  $\phi$ [C(17)–C(18)] are +32.7 and –35.3°. Some of the values of  $\theta$  and  $\phi$  may be compared with those in ring *A* of 2 $\beta$ ,3 $\alpha$ -dichloro-5 $\alpha$ -cholestane (see Geise, Altona & Romers, 1967). In this molecule there is strong repulsion between a chlorine and a carbon atom in positions corresponding to C(19) and C(26) in the baccharis oxide structure. The angle C(17)–C(18)–C(13) in the cholestane derivative is 117.1°, but the two low  $\phi$  values of 40.9 and –42.9° are significantly higher in this molecule. The additional flattening of ring *D* in baccharis oxide can be largely attributed to the presence of an extra methyl group at C(14) and to the transmission of strain from ring *C* arising partly from 1,3-diaxial interaction in this ring and partly from the junction to ring *B*. The connexion with ring *B* prevents a flattening of ring *C* of the same magnitude. Altona & Sundaralingam (1970) have calculated mean values of endocyclic valency angles  $\langle\theta\rangle$  and torsion angles  $\langle|\phi|\rangle$  for three axially substituted cyclohexanes and for cyclohexane itself. The values are listed in Table 8 with those for rings *C* and *D* in baccharis oxide and show the effects of an increasing number of axial substituents and the fusion of rings.

Table 7. *Intramolecular contacts*

(a) Important intramolecular contacts involving carbon and oxygen atoms.

<i>i</i>	<i>j</i>	<i>D<sub>ij</sub></i>	<i>i</i>	<i>j</i>	<i>D<sub>ij</sub></i>
O	C(28)	2.74 Å	C(20)	C(25)	3.17 Å
O	C(30)	2.92	C(27)	C(28)	3.24
C(1)	C(4)	3.03	O	H(282)	2.21
C(1)	C(8)	3.38	C(1)	H(112)	2.48
C(1)	C(11)	2.98	C(2)	H(291)	2.72
C(2)	C(5)	2.88	C(5)	H(81)	2.79
C(2)	C(29)	3.06	C(6)	H(283)	2.60
C(5)	C(8)	2.82	C(6)	H(303)	2.67
C(5)	C(28)	3.36	C(7)	H(152)	2.68
C(6)	C(9)	2.86	C(7)	H(273)	2.67
C(6)	C(28)	3.14	C(7)	H(283)	2.66
C(6)	C(30)	2.90	C(8)	H(263)	2.74
C(7)	C(10)	3.00	C(11)	H(11)	2.60
C(7)	C(15)	3.06	C(11)	H(263)	2.68
C(7)	C(27)	3.05	C(12)	H(281)	2.75
C(7)	C(28)	3.10	C(15)	H(262)	2.73
C(8)	C(12)	2.94	C(16)	H(271)	2.57
C(8)	C(26)	3.10	C(18)	H(271)	2.61
C(9)	C(13)	3.05	C(19)	H(262)	2.66
C(9)	C(27)	3.28	C(20)	H(181)	2.63
C(11)	C(14)	2.98	C(20)	H(242)	2.74
C(11)	C(26)	2.95	C(24)	H(201)	2.65
C(12)	C(27)	3.06	C(25)	H(201)	2.78
C(12)	C(28)	3.18	C(26)	H(81)	2.70
C(13)	C(16)	2.98	C(26)	H(112)	2.59
C(14)	C(17)	3.05	C(26)	H(151)	2.57
C(14)	C(28)	3.36	C(27)	H(71)	2.57
C(15)	C(18)	2.94	C(27)	H(122)	2.65
C(15)	C(26)	2.97	C(27)	H(161)	2.67
C(16)	C(27)	2.93	C(27)	H(182)	2.63
C(17)	C(26)	3.22	C(28)	H(61)	2.69
C(18)	C(20)	3.08	C(28)	H(272)	2.54
C(18)	C(27)	2.95	C(29)	H(22)	2.51
C(19)	C(26)	3.36	C(30)	H(61)	2.59
C(20)	C(24)	3.06			

(b) Shortest intramolecular H···H contacts (<2.25 Å).

<i>i</i>	<i>j</i>	<i>D<sub>ij</sub></i>	<i>i</i>	<i>j</i>	<i>D<sub>ij</sub></i>
H(11)	H(112)	1.94 Å	H(271)	H(161)	2.15 Å
H(22)	H(291)	1.95	H(271)	H(182)	2.13
H(201)	H(242)	2.10	H(272)	H(122)	2.23
H(262)	H(151)	2.12	H(272)	H(281)	2.05
H(262)	H(192)	2.02	H(273)	H(71)	1.97
H(263)	H(81)	2.12	H(281)	H(122)	2.22
H(263)	H(112)	2.11	H(283)	H(61)	1.98

Table 8. *Mean values of endocyclic valency angles  $\langle\theta\rangle$  and magnitudes of torsion angles  $\langle|\phi|\rangle$  in some cyclohexane rings*

		$\langle\theta\rangle$	$\langle \phi \rangle$
*Cyclohexane	calc.	111.0°	56.1°
*Average for 3 axially substituted cyclohexanes with orientation of substituents:			
1 <i>a</i> , 1 <i>e</i> ; 1 <i>a</i> , 1 <i>e</i> , 4 <i>a</i> ; 1 <i>a</i> , 1 <i>e</i> , 4 <i>e</i> .	calc.	111.3	54.7
Baccharis oxide ring <i>C</i>	obs.	111.8	53.1
Baccharis oxide ring <i>D</i>	obs.	112.5	49.0

\* Calculated semi-empirically by Altona & Sundaralingam (1970).

The double-bond system in the C(17) side chain is significantly non-planar,  $\chi^2$  being 5.6 for the plane *pF*. The slight deformation at this site may be described better by giving the dihedral angle of 1.6° between the planes defined by atoms C(20)–H(211)–C(21)–C(22) ( $\chi^2=0.12$ ) and C(21)–C(22)–C(23)–C(24) ( $\chi^2=3.5$ ).

### Packing of molecules

The molecular packing is shown in Fig. 4. Intermolecular contacts are listed in Table 9 within a limit of 0.2 Å greater than the sum of the relevant van der Waals radii. A slightly higher limit of 2.60 Å was used for the H...H contact distances. Contacts occur in pairs equivalent by symmetry and only one in each pair has been given in Table 9. None of the van der Waals distances is much shorter than the normal range, the shortest being C(2)...H(283) at 1 + x, y, z: 2.85 Å vs. 2.97 Å (van der Waals).

Table 9. Important intermolecular contact distances

Distances are included within a limit of 0.2 Å greater than the sum of the relevant van der Waals radii. A limit of 2.60 Å has been used for H...H contacts.  $R_C = 1.80$  Å,  $R_O = 1.36$  Å,  $R_H = 1.17$  Å (Kitaigorodskii, 1961).

Symmetry code			
i	x	y	z
ii	$\frac{1}{2} - x$	$\bar{y}$	$\frac{1}{2} + z$
iii	$\frac{1}{2} + x$	$\frac{1}{2} - y$	$\bar{z}$
iv	$\bar{x}$	$\frac{1}{2} + y$	$\frac{1}{2} - z$
v	1 + x	y	z
vi	$\frac{1}{2} - x$	$\bar{y}$	$-\frac{1}{2} + z$
vii	$\frac{1}{2} + x$	$-\frac{1}{2} - y$	$\bar{z}$
viii	1 - x	$-\frac{1}{2} + y$	$\frac{1}{2} - z$

i	j	$J_{sc}$	$D_{ij}$
C(2)	C(28)	v	3.70 Å
C(22)	C(12)	vii	3.77
C(23)	C(12)	vii	3.71
C(1)	H(283)	v	3.07
C(2)	H(283)	v	2.85
C(20)	H(182)	vii	3.05
C(21)	H(62)	iii	3.01
C(21)	H(182)	vii	3.12
C(22)	H(122)	vii	2.96
C(23)	H(21)	vi	3.05
C(23)	H(122)	vii	3.05
C(23)	H(303)	iii	3.12
O	H(292)	viii	2.63
H(21)	H(283)	v	2.50
H(31)	H(243)	ii	2.59
H(51)	H(162)	iii	2.59
H(72)	H(161)	iii	2.53
H(151)	H(152)	iii	2.45
H(211)	H(62)	iii	2.33
H(231)	H(122)	vii	2.56
H(232)	H(303)	iii	2.58
H(282)	H(233)	ii	2.59

Below the limits given there are 44 intermolecular contacts to atoms all around in the molecule and the molecular coordination number is 12. Contacts involving the outermost part of the C(17) side chain and methyl group C(28) are particularly numerous. Thus the molecules are packed very efficiently in the crystal by intermolecular van der Waals forces. The stereochemistry of the molecule is determined by intramolecular factors.

In addition to the tangent-refinement routine the following programs were used on a UNIVAC 1108:

FOUFU1—Fourier summation and LSFIV4—full-matrix least-squares refinement, both programs written or modified by O. Borgen, B. Mestvedt & J. Finjord [Techn. Reports 52 (1969) and 45 (1966), Inst. for fysikalsk kjemi, NTH]. SCALER—Wilson plot, calculation of  $E$ 's and their distribution and SIGMA2—listing of  $\sum_2$  relations, both programs written by J. Hjortås (Tekn. Rapport 09-RII-70 and 06-RII-69, Inst. for røntgenteknikk, NTH). FSTAT1—weighted averaging of equivalent  $F$ 's and WEIGHT—analysis of weighting of  $F$ 's, written by B. K. Sivertsen (Tekn. Rapport 19-RII-72 and 10-RII-70, Inst. for røntgenteknikk, NTH). TERMVIB2—analysis of rigid-body thermal motion and KORREKS—correction of coordinates and bond lengths according to thermal analysis, written by A. M. Evensen (Tekn. Rapport 13-RII-70 and 14-RII-70, Inst. for røntgenteknikk, NTH).

A grant from Reidar Holmsen og frues legat is gratefully acknowledged.

### References

- ALLEN, F. H. & TROTTER, J. (1970). *J. Chem. Soc. (B)*, pp. 721–727.
- ALTONA, C. & SUNDARALINGAM, M. (1970). *Tetrahedron*, **26**, 925–939.
- ANTHONSEN, T., BRUUN, T., HEMMER, E., HOLME, D., LAMVIK, A., SUNDE, E. & SØRENSEN, N. A. (1970). *Acta Chem. Scand.* **24**, 2479–2488.
- BIRNBAUM, K. B. & FERGUSON, G. (1969). *Acta Cryst.* **B25**, 720–730.
- BJÄMER, K., FERGUSON, G. & MELVILLE, R. D. (1968). *Acta Cryst.* **B24**, 855–865.
- CROMER, D. T. & LIBERMAN, D. (1970). University of California Report LA-4403, UC-34. Los Alamos Scientific Laboratory, California.
- CRUICKSHANK, D. W. J. (1956). *Acta Cryst.* **9**, 757–758.
- DOYLE, P. A. & TURNER, P. S. (1968). *Acta Cryst.* **A24**, 390–397.
- GEISE, H. J., ALTONA, C. & ROMERS, C. (1967). *Tetrahedron*, **23**, 439–463.
- GERMAIN, G., MAIN, P. & WOOLFSON, M. M. (1971). *Acta Cryst.* **A27**, 368–376.
- GERMAIN, G. & WOOLFSON, M. M. (1968). *Acta Cryst.* **B24**, 91–96.
- HAUPTMAN, H. & KARLE, J. (1953). *Solution of the Phase Problem. I. The Centrosymmetric Crystal*. A.C.A. Monograph No. 3. Pittsburgh: Polycrystal Book Service.
- KARLE, J. & HAUPTMAN, H. (1956). *Acta Cryst.* **9**, 635–651.
- KARLE, J. & KARLE, I. L. (1966). *Acta Cryst.* **21**, 849–859.
- KITAIGORODSKII, A. I. (1961). *Organic Chemical Crystallography*. New York: Consultants Bureau.
- KLYNE, W. & PRELOG, V. (1960). *Experientia*, **16**, 521–523.
- KOYAMA, H. & NAKAI, H. (1970). *J. Chem. Soc. (B)*, pp. 546–554.
- MO, F. (1972). Tekn. Rapport 17-RII-72. Inst. for røntgenteknikk, NTH, Trondheim.
- MO, F., ANTHONSEN, T. & BRUUN, T. (1972). *Acta Chem. Scand.* **26**, 1287–1288.
- SCHOMAKER, V. & TRUEBLOOD, K. N. (1968). *Acta Cryst.* **B24**, 63–76.

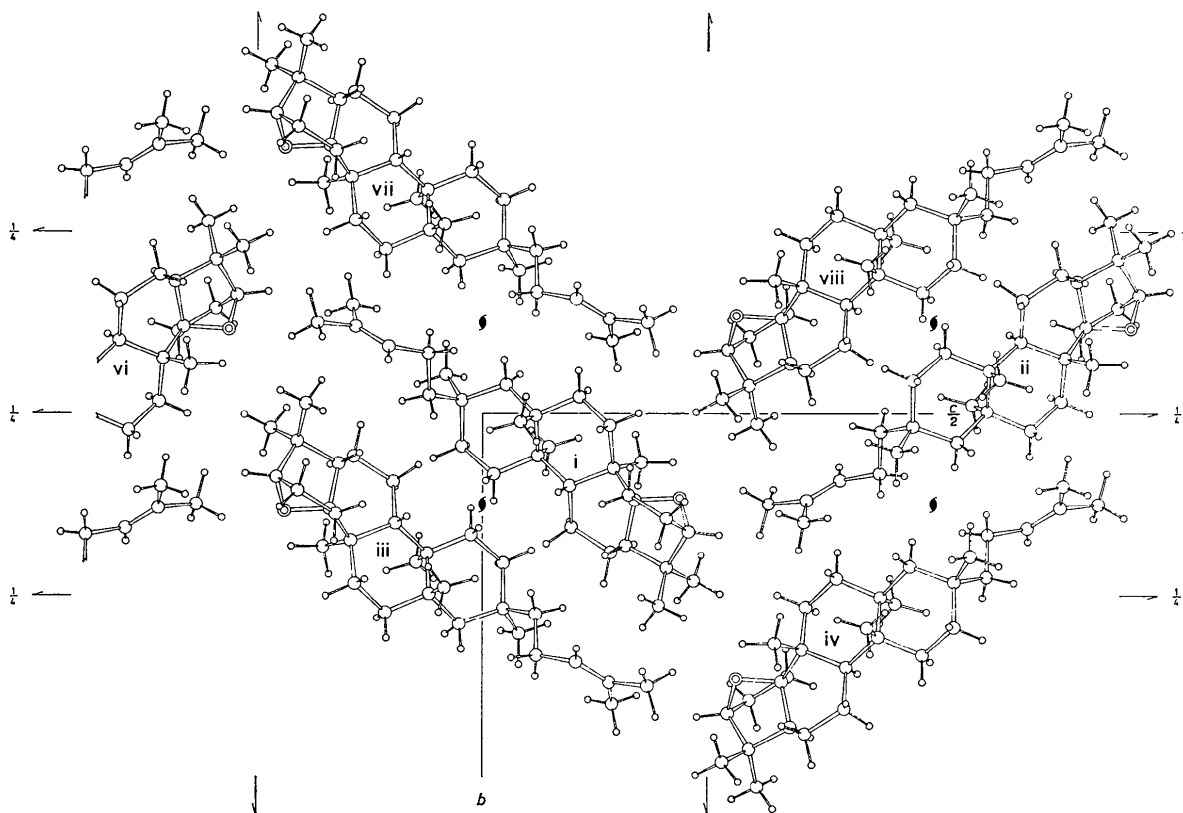


Fig. 4. Packing of molecules projected on (100). For explanation of symmetry code see Table 9.

SINGH, P. & AHMED, F. R. (1969). *Acta Cryst.* **B25**, 2401–2408.  
 STEWART, R. F., DAVIDSON, E. R. & SIMPSON, W. T. (1965). *J. Chem. Phys.* **42**, 3175–3178.

SUOKAS, T. & HASE, T. (1971). *Acta Chem. Scand.* **25**, 2359–2360.  
 ZACHARIASEN, W. H. (1963). *Acta Cryst.* **16**, 1139–1144.  
 ZACHARIASEN, W. H. (1965). *Acta Cryst.* **18**, 714–716.